

Observation of Critical Phenomena in Parity-Time-Symmetric Quantum Dynamics

Lei Xiao,^{1,2} Kunkun Wang,¹ Xiang Zhan,¹ Zhihao Bian,¹ Kohei Kawabata,³
Masahito Ueda,^{3,4} Wei Yi,^{5,6} and Peng Xue^{1,*}

¹Beijing Computational Science Research Center, Beijing 100084, China

²Department of Physics, Southeast University, Nanjing 211189, China

³Department of Physics, University of Tokyo, 7-3-1 Hongo, Bunkyo-ku, Tokyo 113-0033, Japan

⁴RIKEN Center for Emergent Matter Science (CEMS), Wako, Saitama 351-0198, Japan

⁵CAS Key Laboratory of Quantum Information, University of Science and Technology of China, Hefei 230026, China

⁶CAS Center For Excellence in Quantum Information and Quantum Physics, Hefei 230026, China



(Received 29 October 2018; published 3 December 2019)

We experimentally simulate nonunitary quantum dynamics using a single-photon interferometric network and study the information flow between a parity-time- (\mathcal{PT} -)symmetric non-Hermitian system and its environment. We observe oscillations of quantum-state distinguishability and complete information retrieval in the \mathcal{PT} -symmetry-unbroken regime. We then characterize in detail critical phenomena of the information flow near the exceptional point separating the \mathcal{PT} -unbroken and \mathcal{PT} -broken regimes, and demonstrate power-law behavior in key quantities such as the distinguishability and the recurrence time. We also reveal how the critical phenomena are affected by symmetry and initial conditions. Finally, introducing an ancilla as an environment and probing quantum entanglement between the system and the environment, we confirm that the observed information retrieval is induced by a finite-dimensional entanglement partner in the environment. Our work constitutes the first experimental characterization of critical phenomena in \mathcal{PT} -symmetric nonunitary quantum dynamics.

DOI: [10.1103/PhysRevLett.123.230401](https://doi.org/10.1103/PhysRevLett.123.230401)

Parity-time- (\mathcal{PT} -)symmetric non-Hermitian systems feature unconventional properties in synthetic systems ranging from classical optical systems [1–13] and microwave cavities [14–16] to quantum gases [17] and single photons [18,19]. In these systems, the spectrum is entirely real in the \mathcal{PT} -symmetry-unbroken regime, in contrast to the regime with spontaneously broken \mathcal{PT} symmetry [20–22]. As a result, the dynamics is drastically different in the \mathcal{PT} -symmetry-unbroken and \mathcal{PT} -symmetry-broken regimes, and dynamical criticality occurs at the boundary between the two regimes [23,24]. In previous experiments, such unconventional dynamical properties as well as signatures of the \mathcal{PT} -transition point, or the exceptional point, were observed in classical \mathcal{PT} -symmetric systems with balanced gain and loss [3,7–10,25]. Whereas quantum systems with passive \mathcal{PT} symmetry were realized recently [17,18], critical phenomena in \mathcal{PT} -symmetric quantum dynamics are yet to be experimentally explored. Understanding these critical phenomena in the quantum regime provides an important perspective for the study of open quantum systems and is useful for applications in quantum information.

A paradigmatic example of \mathcal{PT} -symmetric nonunitary dynamics in the context of open quantum systems is the reversible-irreversible criticality in the information flow between a system and its environment [26]. Here, information lost to the environment can be fully retrieved when

the system is in the \mathcal{PT} -symmetry-unbroken regime because of the existence of a finite-dimensional entanglement partner in the environment protected by \mathcal{PT} symmetry. In contrast, the information flow is irreversible when the system spontaneously breaks \mathcal{PT} symmetry. Close to the exceptional point, physical quantities such as distinguishability between time-evolved states and the recurrence time of the distinguishability exhibit power-law behavior.

In this Letter, we simulate \mathcal{PT} -symmetric nonunitary quantum dynamics using a single-photon interferometric network, and experimentally investigate the critical phenomena in the information flow close to the exceptional point. To extract critical phenomena from nonunitary dynamics, a faithful characterization of the long-time dynamics is necessary. This poses a serious experimental challenge, because maintaining and probing coherent dynamics in the long-time regime is difficult. We overcome this difficulty by directly implementing nonunitary time-evolution operators at any given time, and simulate the nonunitary quantum dynamics by performing nonunitary gate operations on the initial state. We then perform quantum-state tomography on the time-evolved state, which enables us to confirm the critical power-law scaling in various physical quantities. Since our experimental protocol is general enough to implement a broad class of nonunitary operators, we are able to examine in detail the

role of symmetry and initial states on nonunitary quantum dynamics driven by a series of related non-Hermitian Hamiltonians. Furthermore, introducing ancillary degrees of freedom as the environment, we explicitly demonstrate oscillations in the quantum entanglement between the system and the environment in the unitary dynamics of the combined system-environment quantum system. This demonstrates the existence of a finite-dimensional entanglement partner in the environment, which is responsible for the information retrieval. Our work is the first experiment to characterize critical phenomena in \mathcal{PT} -symmetric nonunitary quantum dynamics, and opens up an avenue toward simulating the \mathcal{PT} -symmetric dynamics in synthetic quantum systems.

Experimental setup.—To simulate the dynamics of a two-level \mathcal{PT} -symmetric system, we encode basis states in the horizontal and vertical polarizations of a single photon, with $|H\rangle = (1, 0)^T$ and $|V\rangle = (0, 1)^T$. We generate heralded single photons via type-I spontaneous parametric down-conversion, with one photon serving as a trigger and the other as a signal. The signal photon is then projected into the initial state $|H\rangle$ or $|V\rangle$ with a polarizing beam splitter (PBS) and a half-wave plate (HWP), and is sent to the interferometric network as illustrated in Fig. 1.

Experimentally, instead of implementing a non-Hermitian Hamiltonian, we directly realize the time-evolution operator U at any given time t and access time-evolved states by enforcing U on the initial state. As illustrated in Fig. 1, this is achieved by decomposing U according to

$$U = R_2(\theta_2, \varphi_2)L(\theta_H, \theta_V)R_1(\theta_1, \varphi_1), \quad (1)$$

where the rotation operator $R_j(\theta_j, \varphi_j)$ ($j = 1, 2$) is realized using a quarter-wave plate (QWP) at φ_j and a HWP at θ_j , and the polarization-dependent loss operator L is realized by a combination of two beam displacers (BDs) and two HWPs with setting angles θ_H and θ_V [27].

Here, the setting angles $\{\theta_j, \varphi_j, \theta_H, \theta_V\}$ of wave plates are determined numerically for each given time t , such that $U = e^{-i\hat{H}_{\text{eff}}t}$. In our experiment, the effective non-Hermitian Hamiltonian is given by

$$\hat{H}_{\text{eff}} = \hat{\sigma}_x + ia(\hat{\sigma}_z - \hat{1}), \quad (2)$$

where $\hat{\sigma}_{x(z)}$ are the standard Pauli operators, and $\hat{1}$ is the identity operator. The non-Hermitian Hamiltonian \hat{H}_{eff} possesses passive \mathcal{PT} symmetry, which can be easily mapped to a \mathcal{PT} -symmetric Hamiltonian $\hat{H}_{\mathcal{PT}}$ with balanced gain and loss, with $\hat{H}_{\mathcal{PT}} = \hat{H}_{\text{eff}} + ia\hat{1}$. Here, $a > 0$ controls non-Hermiticity, and the Hamiltonian becomes Hermitian for $a = 0$; the system is in the \mathcal{PT} -symmetry-unbroken (\mathcal{PT} -symmetry-broken) regime for $0 < a < 1$ ($a > 1$), with the exceptional point located at $a = 1$.

The nonunitary dynamics of the system is captured by the time-dependent density matrix [26,28]

$$\rho_{1,2}(t) = \frac{e^{-i\hat{H}_{\mathcal{PT}}t}\rho_{1,2}(0)e^{i\hat{H}_{\mathcal{PT}}^\dagger t}}{\text{Tr}[e^{-i\hat{H}_{\mathcal{PT}}t}\rho_{1,2}(0)e^{i\hat{H}_{\mathcal{PT}}^\dagger t}]}, \quad (3)$$

with the initial density matrices $\rho_{1(2)}(0) = |H(V)\rangle\langle H(V)|$. Note that applying \hat{H}_{eff} or $\hat{H}_{\mathcal{PT}}$ in Eq. (3) would give the same time-dependent matrices. Experimentally, we construct

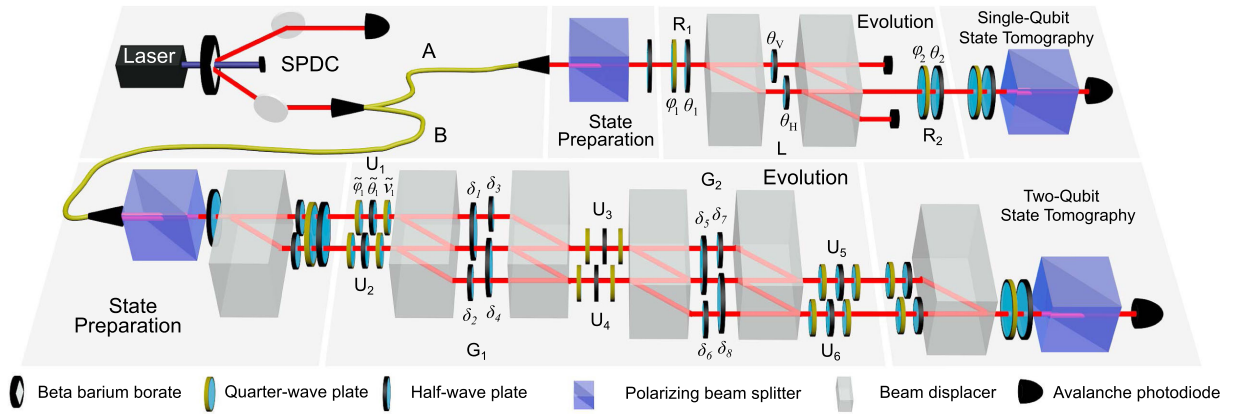


FIG. 1. Experimental setup. A photon pair is created via spontaneous parametric down-conversion (SPDC). One of the photons serves as a trigger, the other is projected into the polarization state $|H\rangle$ or $|V\rangle$ with a polarizing beam splitter (PBS) and a half-wave plate (HWP), and then goes through various optical elements. Upper layer: the experimental setup for the nonunitary dynamics of a single-qubit \mathcal{PT} -symmetric system. Lower layer: experimental setup for the unitary dynamics of a two-qubit system, where the two qubits are encoded in polarization and spatial degrees of freedom. To prepare the initial state of a two-qubit system, heralded single photons pass through a PBS and a HWP with certain setting angles and are split by a birefringent calcite beam displacer (BD) into two parallel spatial modes: upper and lower modes. After passing through wave plates inserted into different spatial modes, the photons are prepared in the state $|\bar{0}\rangle$ or $|\bar{1}\rangle$ (see the main text for the definition). We construct the time-dependent density matrices by performing quantum-state tomography for both of these states.

the density matrix at any given time t via quantum-state tomography after signal photons passed through the interferometric setup. Essentially, we measure the probabilities of photons in the bases $\{|H\rangle, |V\rangle, |P_+\rangle = (|H\rangle + |V\rangle)/\sqrt{2}, |P_-\rangle = (|H\rangle - i|V\rangle)/\sqrt{2}\}$ through a combination of QWP, HWP, and PBS, and then perform a maximum-likelihood estimation of the density matrix. The outputs are recorded in synchronization with trigger photons. Typical measurements yield a maximum of 18 000 photon counts over 3 s.

Measuring distinguishability.—We characterize information flowing into and out of the system via the trace distance defined by

$$D[\rho_1(t), \rho_2(t)] = \frac{1}{2} \text{Tr}|\rho_1(t) - \rho_2(t)|, \quad (4)$$

with $|A| = \sqrt{A^\dagger A}$. The trace distance D measures the distinguishability of the two quantum states characterized by $\rho_1(t)$ and $\rho_2(t)$. An increase in the distinguishability signifies information backflow from the environment, whereas a monotonic decrease means irreversible information flow to the environment [26,29].

In Fig. 2, we show the time evolution of the distinguishability when the system is in the \mathcal{PT} -symmetry-unbroken regime with $a < 1$. For comparison, we also show the case of a unitary evolution with $a = 0$. As illustrated in Figs. 2(a)–2(c), $D(t)$ oscillates in time for $a < 1$, suggesting complete information retrieval with the initial trace distance fully restored periodically. The period of the oscillation T , or the recurrence time, increases as the

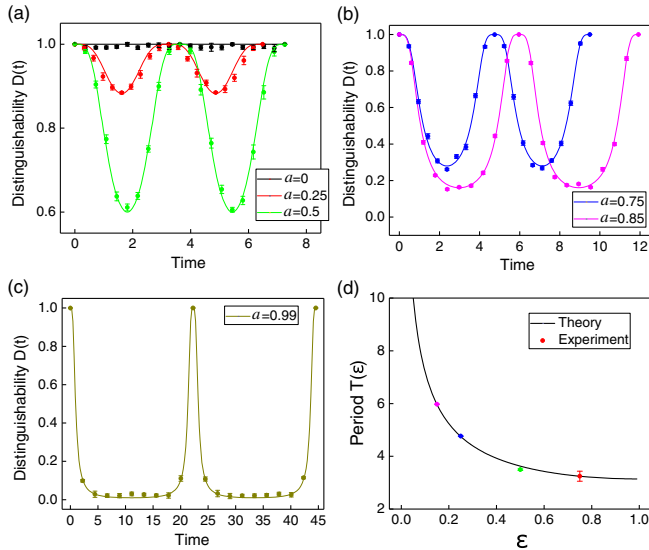


FIG. 2. Information retrieval in the \mathcal{PT} -symmetry-unbroken regime. (a)–(c) Oscillations of the distinguishability $D(t)$ for $a < 1$, between the two time-evolved states starting from $|H\rangle$ and $|V\rangle$. Dots with error bars represent the experimental results, while the curves show the theoretical predictions. (d) Recurrence time T of the distinguishability as a function of $\varepsilon = 1 - a$.

system approaches the exceptional point. We extract the recurrence time by fitting the experimental data with a Fourier series. As shown in Fig. 2(d), the recurrence time agrees well with the analytic expression $T = \pi/\sqrt{1 - a^2}$ [26]. In the limit $\varepsilon \rightarrow 0$ with $\varepsilon = 1 - a$, the recurrence time diverges as $T \sim \varepsilon^{-1/2}$.

In Fig. 3(a), we show the time evolution of the distinguishability when the system is in the \mathcal{PT} -symmetry-broken regime with $a > 1$. Here, the distinguishability decays exponentially in time. Fitting the experimental data using $D(t) = D(0)e^{-t/\tau}$, where $D(0)$ is a constant and τ is the relaxation time, we find that the relaxation time increases as the system approaches the exceptional point. As shown in Fig. 3(b), the measured τ agrees excellently with the analytical result $\tau = 1/2\sqrt{a^2 - 1}$ [26], which also diverges with a power-law scaling $\tau \sim |\varepsilon|^{-1/2}$ as $\varepsilon \rightarrow 0$.

Finally, at the exceptional point ($a = 1$), the distinguishability exhibits power-law behavior in the long-time limit. As illustrated in Fig. 4(a), the long-time behavior of the distinguishability agrees well with the theoretical prediction $D(t) \sim t^{-2}$ [26]. Importantly, the observed critical phenomena depend not on the details of the system but on the order of the exceptional point, which signifies their universality [23,24]. We note that the measurement suffers from a relatively larger systematic error at long times due to the small $D(t)$.

Symmetry and initial states.—Since our experimental protocol is quite general and capable of implementing a broad class of nonunitary operators [27], we are able to investigate the role of symmetry and initial states on the information flow and critical phenomena. In particular, we experimentally simulate nonunitary dynamics governed by (i) $\hat{H}_T = \hat{\sigma}_x + ia\hat{\sigma}_y$ and (ii) $\hat{H} = \hat{\sigma}_x + (c + ia)\hat{\sigma}_z$. Whereas \hat{H}_T has time-reversal symmetry $\mathcal{T}\hat{H}_T\mathcal{T}^{-1} = \hat{H}_T$ with complex conjugation \mathcal{T} , \hat{H} has no relevant symmetries for $a \neq 0$ and $c \neq 0$.

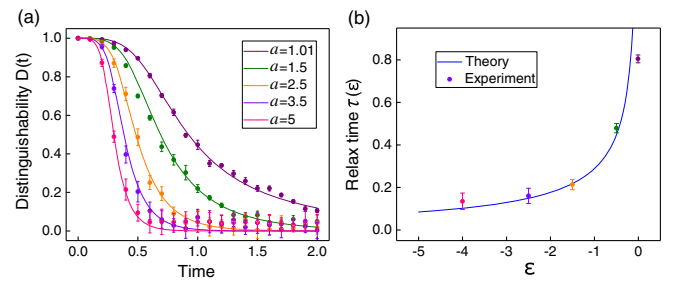


FIG. 3. Irreversible information flow to the environment in the \mathcal{PT} -symmetry-broken regime. (a) Decay of the distinguishability in the \mathcal{PT} -broken regime with different coefficients $a > 1$. (b) Relaxation time τ of the distinguishability as a function of $\varepsilon = 1 - a$. The blue solid curve shows the theoretical result $\tau = 1/2\sqrt{a^2 - 1}$. The relaxation time is determined by fitting the experimental results (dots with error bars) to an exponential function.

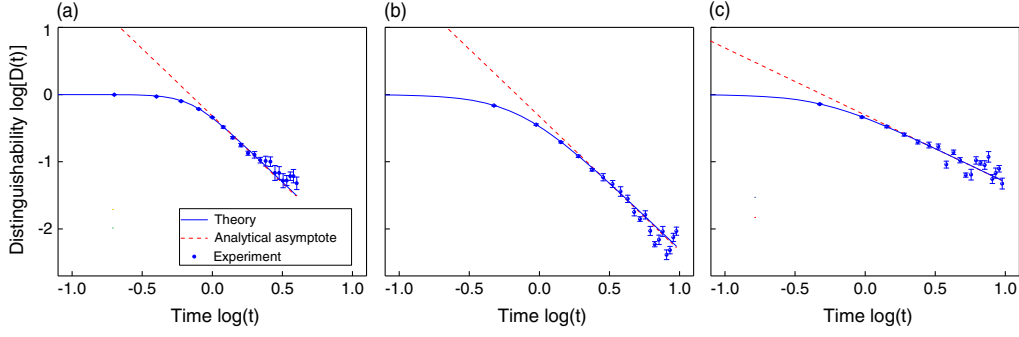


FIG. 4. (a) Power-law behavior of the distinguishability $D(t) \sim t^{-2}$ of the \mathcal{PT} -symmetric system for initial states $\{|H\rangle, |V\rangle\}$. (b),(c) Power-law behavior of the distinguishability of the time-reversal-symmetric system at the exceptional point $a = 1$ for initial states (b) $(|H\rangle \pm |V\rangle)/\sqrt{2}$ and (c) $\{|H\rangle, |V\rangle\}$. The power-law behaviors $D(t) \sim t^{-2}$ in (b) and $D(t) \sim t^{-1}$ in (c) demonstrate the dependence of the critical phenomena on the initial state. In the long-time limit, the experimentally measured distinguishability agrees well with theoretical asymptotes. The blue solid curves show the theoretical prediction, and the red dashed lines indicate their asymptotes.

We first study dynamics under \hat{H}_T with different parameters and initial states $(|H\rangle \pm |V\rangle)/\sqrt{2}$. Since eigenenergies of \hat{H}_T are given as $\pm\sqrt{1-a^2}$, the exceptional point is located at $a = 1$. As shown in Fig. 4(b), the same critical phenomena emerge under time-reversal symmetry: information is retrieved only in the symmetry-unbroken regime ($0 < a < 1$) [27], and the critical scaling is still $D(t) \sim t^{-2}$. However, when we choose the initial states $\{|H\rangle, |V\rangle\}$, the critical scaling at the exceptional point is now $D(t) \sim t^{-1}$, as illustrated in Fig. 4(c). This new universality arises because $|H\rangle$ is one of the eigenstates of \hat{H}_T . We note that the same scaling relation can be realized under $\hat{H}_{\mathcal{PT}}$ with the initial states $(|H\rangle \pm i|V\rangle)/\sqrt{2}$ since $(|H\rangle - i|V\rangle)/\sqrt{2}$ is one of the eigenstates of $\hat{H}_{\mathcal{PT}}$. For the dynamics governed by \hat{H} , however, the lack of symmetry therein prevents the information retrieval and the distinguishability decays in time just as in the symmetry-broken cases [27].

\mathcal{PT} dynamics embedded in a two-qubit system.—To unveil the origin of the information retrieval, we embed the \mathcal{PT} dynamics into a larger Hilbert space by introducing an ancilla as the environment [26,30]. The combined two-qubit system is governed by the Hermitian Hamiltonian

$$\hat{H}_{\text{tot}} = \hat{1}^a \otimes \hat{H}_s + \hat{\sigma}_y^a \otimes \hat{V}_s, \quad (5)$$

where $\hat{1}^a$ and $\hat{\sigma}_y^a$ act on the ancilla; \hat{H}_s and \hat{V}_s act on the \mathcal{PT} -symmetric system with

$$\hat{H}_s = c^{-1}(\hat{H}_{\mathcal{PT}}\hat{\eta}^{-1} + \hat{\eta}\hat{H}_{\mathcal{PT}}), \quad (6)$$

$$\hat{V}_s = ic^{-1}(\hat{H}_{\mathcal{PT}} - \hat{H}_{\mathcal{PT}}^\dagger). \quad (7)$$

Here, the non-Hermitian Hamiltonian satisfies pseudo-Hermiticity with $\hat{\eta}\hat{H}_{\mathcal{PT}} = \hat{H}_{\mathcal{PT}}^\dagger\hat{\eta}$ and

$$\hat{\eta} = \frac{1}{\sqrt{1-a^2}} \begin{pmatrix} 1 & -ia \\ ia & 1 \end{pmatrix},$$

where we have $c = \sum_j 1/\lambda_j$ with the eigenvalues λ_j of $\hat{\eta}$. Whereas the unitary time evolution of the two-qubit system is driven by the Hermitian Hamiltonian \hat{H}_{tot} , the effective time evolution of the subsystem is nonunitary and driven by $\hat{H}_{\mathcal{PT}}$ under a postselection on the ancilla.

Experimentally, the ancillary degrees of freedom are encoded in two independent spatial modes of the signal photons $\{|u\rangle, |d\rangle\}$. Thus, the bases of two-qubit states can be written as $\{|u\rangle|H\rangle = (1, 0, 0, 0)^T, |u\rangle|V\rangle = (0, 1, 0, 0)^T, |d\rangle|H\rangle = (0, 0, 1, 0)^T, |d\rangle|V\rangle = (0, 0, 0, 1)^T\}$. The unitary operator U_{tot} can be decomposed into [31–34]

$$U_{\text{tot}} = \begin{pmatrix} U_5 & 0 \\ 0 & U_6 \end{pmatrix} G_2 \begin{pmatrix} U_3 & 0 \\ 0 & U_4 \end{pmatrix} G_1 \begin{pmatrix} U_1 & 0 \\ 0 & U_2 \end{pmatrix}, \quad (8)$$

where U_j ($j = 1, \dots, 6$) are unitary single-qubit rotation operators, and G_1 and G_2 are two-qubit operators. While U_j is implemented using a set of sandwiched wave plates with the configuration QWP (at $\tilde{\phi}_j$)-HWP (at $\tilde{\theta}_j$)-QWP (at $\tilde{\nu}_j$), G_1 and G_2 are realized via a combination of BDs and HWPs by setting angles δ_j ($j = 1, \dots, 8$) as illustrated in Fig. 1 [27]. Similar to the single-qubit case, these setting angles are determined numerically to ensure that Eq. (8) yields the correct time-evolution operator $U_{\text{tot}} = e^{-i\hat{H}_{\text{tot}}t}$.

We then construct the final state at any given time t through quantum-state tomography. This is achieved through measurements of probabilities of photons in 16 bases given by $\{|u\rangle, |d\rangle, |S_+\rangle, |S_-\rangle\} \otimes \{|H\rangle, |V\rangle, |P_+\rangle, |P_-\rangle\}$ with $|S_+\rangle = (|u\rangle + |d\rangle)/\sqrt{2}$, and $|S_-\rangle = (|u\rangle - |d\rangle)/\sqrt{2}$. From the measured correlations, we calculate density matrices of the system and the ancilla from

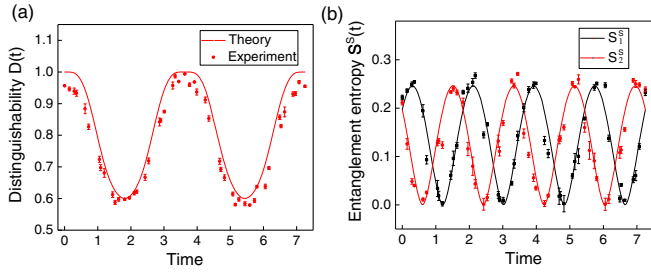


FIG. 5. \mathcal{PT} dynamics embedded in a two-qubit system with $a = 0.5$. (a) Quantum oscillations of the distinguishability. (b) Entanglement entropy between the \mathcal{PT} -symmetric system and its ancilla, which oscillates with half the period of that of the distinguishability.

$$\rho_j^s(t) = \text{Tr}_a[\rho_j^{\text{tot}}(t)], \quad \rho_j^a(t) = \text{Tr}_s[\rho_j^{\text{tot}}(t)] \quad (j = 1, 2). \quad (9)$$

On the other hand, the density matrix of the \mathcal{PT} -symmetric system is

$$\rho_j^{\mathcal{PT}}(t) = \mathcal{N} \text{Tr}_a[(|u\rangle\langle u| \otimes \hat{1})\rho_j^{\text{tot}}(t)(|u\rangle\langle u| \otimes \hat{1})^\dagger], \quad (10)$$

with a normalization constant \mathcal{N} .

For comparison with the single-qubit case, we calculate the distinguishability between two time-evolved states $\rho_1^{\mathcal{PT}}(t)$ and $\rho_2^{\mathcal{PT}}(t)$. We choose the initial states as $|\bar{0}\rangle \propto |u\rangle|H\rangle + |d\rangle \otimes \hat{\eta}|H\rangle$ and $|\bar{1}\rangle \propto |u\rangle|V\rangle + |d\rangle \otimes \hat{\eta}|V\rangle$. As illustrated in Fig. 5(a), the information retrieval can be observed in the \mathcal{PT} -symmetric system.

Importantly, the existence of a hidden entangled partner behind the information retrieval is revealed through the entanglement entropy between the system and the ancilla. The time-dependent entanglement entropy between the \mathcal{PT} -symmetric system and its ancilla is calculated as

$$S_j^s(t) = -\text{Tr}[\rho_j^s(t) \log \rho_j^s(t)]. \quad (11)$$

In Fig. 5(b), we show the experimental results of the entanglement entropy for the two different initial states. The entanglement entropy oscillates with half the period of that of the distinguishability, which agrees with the theoretical predictions [26] and confirms the exchange of quantum information between the system and the environment during the \mathcal{PT} dynamics.

Conclusion.—We have experimentally simulated \mathcal{PT} -symmetric quantum dynamics using single-photon interferometric networks. Enforcing nonunitary gate operations on photons and performing quantum-state tomography, we have reconstructed a time-dependent density matrix of the \mathcal{PT} dynamics at arbitrary times. This enables us to characterize critical phenomena close to the \mathcal{PT} -transition point and reveal a hidden entanglement partner in the environment. Our work is the first experimental demonstration of critical phenomena in \mathcal{PT} -symmetric nonunitary quantum dynamics. We expect that critical phenomena

associated with higher-order exceptional points can also be probed using a similar approach.

This work has been supported by the National Natural Science Foundation of China (Grants No. 11674056, No. U1930402, No. 11522545, and No. 11974331). L. X. is supported by Postgraduate Research & Practice Innovation Program of Jiangsu Province (KYCX18_0056). K. K. is supported by the Japan Society for the Promotion of Science (JSPS) through the Program for Leading Graduate Schools (ALPS) and KAKENHI Grant No. JP19J21927. M. U. acknowledges support by KAKENHI, Grants No. JP18H01145 and No. JP15H05855 from the JSPS. W. Y. acknowledges support from the National Key Research and Development Program of China (Grants No. 2016YFA0301700 and No. 2017YFA0304100).

*gnep.eux@gmail.com

- [1] A. Guo, G. J. Salamo, D. Duchesne, R. Morandotti, M. Volatier-Ravat, V. Aimez, G. A. Siviloglou, and D. N. Christodoulides, Observation of \mathcal{PT} -Symmetry Breaking in Complex Optical Potentials, *Phys. Rev. Lett.* **103**, 093902 (2009).
- [2] Y. D. Chong, L. Ge, and A. D. Stone, \mathcal{PT} -Symmetry Breaking and Laser-Absorber Modes in Optical Scattering Systems, *Phys. Rev. Lett.* **106**, 093902 (2011).
- [3] A. Regensburger, C. Bersch, M.-A. Miri, G. Onishchukov, D. N. Christodoulides, and U. Peschel, Parity-time synthetic photonic lattices, *Nature (London)* **488**, 167 (2012).
- [4] M. Liertzer, L. Ge, A. Cerjan, A. D. Stone, H. E. Türeci, and S. Rotter, Pump-Induced Exceptional Points in Lasers, *Phys. Rev. Lett.* **108**, 173901 (2012).
- [5] M. Brandstetter, M. Liertzer, C. Deutsch, P. Klang, J. Schöberl, H. E. Türeci, G. Strasser, K. Unterrainer, and S. Rotter, Reversing the pump dependence of a laser at an exceptional point, *Nat. Commun.* **5**, 4034 (2014).
- [6] S. Weimann, M. Kremer, Y. Plotnik, Y. Lumer, S. Nolte, K. G. Makris, M. Segev, M. C. Rechtsman, and A. Szameit, Topologically protected bound states in photonic parity-time-symmetric crystals, *Nat. Mater.* **16**, 433 (2017).
- [7] H. Hodaie, A. U. Hassan, S. Wittek, H. Garcia-Gracia, R. El-Ganainy, D. N. Christodoulides, and M. Khajavikhan, Enhanced sensitivity at higher-order exceptional points, *Nature (London)* **548**, 187 (2017).
- [8] C. E. Rüter, K. G. Makris, R. El-Ganainy, D. N. Christodoulides, M. Segev, and D. Kip, Observation of parity-time symmetry in optics, *Nat. Phys.* **6**, 192 (2010).
- [9] M. Wimmer, M. A. Miri, D. N. Christodoulides, and U. Peschel, Observation of Bloch oscillations in complex \mathcal{PT} -symmetric photonic lattices, *Sci. Rep.* **5**, 17760 (2015).
- [10] L. Feng, Y.-L. Xu, W. S. Fegadolli, M.-H. Lu, J. E. B. Oliveira, V. R. Almeida, Y.-F. Chen, and A. Scherer, Experimental demonstration of a unidirectional reflectionless parity-time metamaterial at optical frequencies, *Nat. Mater.* **12**, 108 (2013).
- [11] B. Peng, Ş. K. Özdemir, S. Rotter, H. Yilmaz, M. Liertzer, F. Monifi, C. M. Bender, F. Nori, and L. Yang, Loss-induced suppression and revival of lasing, *Science* **346**, 328 (2014).

- [12] J. Zhang, B. Peng, Ş. K. Özdemir, K. Pichler, D. O. Krimer, G. Zhao, F. Nori, Y. X. Liu, S. Rotter, and L. Yang, A phonon laser operating at an exceptional point, *Nat. Photonics* **12**, 479 (2018).
- [13] Ş. K. Özdemir, S. Rotter, F. Nori, and L. Yang, Parity-time symmetry and exceptional points in photonics, *Nat. Mater.* **18**, 783 (2019).
- [14] B. Peng, Ş. K. Özdemir, F. Lei, F. Monifi, M. Gianfreda, G. L. Long, S. Fan, F. Nori, C. M. Bender, and L. Yang, Parity-time-symmetric whispering-gallery microcavities, *Nat. Phys.* **10**, 394 (2014).
- [15] C. Poli, M. Bellec, U. Kuhl, F. Mortessagne, and H. Schomerus, Selective enhancement of topologically induced interface states in a dielectric resonator chain, *Nat. Commun.* **6**, 6710 (2015).
- [16] Z.-P. Liu, J. Zhang, Ş. K. Özdemir, B. Peng, H. Jing, X.-Y. Lü, C.-W. Li, L. Yang, F. Nori, and Y.-X. Liu, Metrology with \mathcal{PT} -Symmetric Cavities: Enhanced Sensitivity Near the \mathcal{PT} -Phase Transition, *Phys. Rev. Lett.* **117**, 110802 (2016).
- [17] J. Li, A. K. Harter, J. Liu, L. de Melo, Y. N. Joglekar, and L. Luo, Observation of parity-time symmetry breaking transitions in a dissipative Floquet system of ultracold atoms, *Nat. Commun.* **10**, 855 (2019).
- [18] L. Xiao, X. Zhan, Z. H. Bian, K. K. Wang, X. Zhang, X. P. Wang, J. Li, K. Mochizuki, D. Kim, N. Kawakami, W. Yi, H. Obuse, B. C. Sanders, and P. Xue, Observation of topological edge states in parity-time-symmetric quantum walks, *Nat. Phys.* **13**, 1117 (2017).
- [19] K. K. Wang, X. Z. Qiu, L. Xiao, X. Zhan, Z. H. Bian, W. Yi, and P. Xue, Observation of emergent momentum-time skyrmions in parity-time-symmetric non-unitary quench dynamics, *Nat. Commun.* **10**, 2293 (2019).
- [20] C. M. Bender and S. Boettcher, Real Spectra in Non-Hermitian Hamiltonians Having \mathcal{PT} Symmetry, *Phys. Rev. Lett.* **80**, 5243 (1998).
- [21] C. M. Bender, D. C. Brody, and H. F. Jones, Complex Extension of Quantum Mechanics, *Phys. Rev. Lett.* **89**, 270401 (2002).
- [22] C. M. Bender, Making sense of non-Hermitian Hamiltonians, *Rep. Prog. Phys.* **70**, 947 (2007).
- [23] W. D. Heiss, The physics of exceptional points, *J. Phys. A* **45**, 444016 (2012).
- [24] R. El-Ganainy, K. G. Makris, M. Khajavikhan, Z. H. Mussilmani, S. Rotter, and D. N. Christodoulides, Non-Hermitian physics and \mathcal{PT} symmetry, *Nat. Phys.* **14**, 11 (2018).
- [25] H. Xu, D. Mason, L. Jiang, and J. G. E. Harris, Topological energy transfer in an optomechanical system with exceptional points, *Nature (London)* **537**, 80 (2016).
- [26] K. Kawabata, Y. Ashida, and M. Ueda, Information Retrieval and Criticality in Parity-Time-Symmetric Systems, *Phys. Rev. Lett.* **119**, 190401 (2017).
- [27] See Supplemental Materials at <http://link.aps.org/supplemental/10.1103/PhysRevLett.123.230401> for details on experimental implementation of non-unitary dynamics and two-qubit evolution, experimental observations of critical phenomena in non-unitary dynamics with other symmetries, and experimental results of quantum mutual information.
- [28] D. C. Brody and E.-M. Graefe, Mixed-State Evolution in the Presence of Gain and Loss, *Phys. Rev. Lett.* **109**, 230405 (2012).
- [29] H.-P. Breuer, E.-M. Laine, and J. Piilo, Measure for the Degree of Non-Markovian Behavior of Quantum Processes in Open Systems, *Phys. Rev. Lett.* **103**, 210401 (2009).
- [30] U. Günther and B. F. Samsonov, Naimark-Dilated \mathcal{PT} -Symmetric Brachistochrone, *Phys. Rev. Lett.* **101**, 230404 (2008).
- [31] G. W. Stewart, On the perturbation of pseudo-inverses, projections and linear least squares problems, *SIAM Rev.* **19**, 634 (1977).
- [32] G. W. Stewart, Computing the CS decomposition of a partitioned orthonormal matrix, *Numer. Math.* **40**, 297 (1982).
- [33] C. C. Paige and M. Wei, History and generality of the CS decomposition, *Linear Algebra Appl.* **208–209**, 303 (1994).
- [34] J. A. Izaac, X. Zhan, Z. H. Bian, K. K. Wang, J. Li, J. B. Wang, and P. Xue, Centrality measure based on continuous-time quantum walks and experimental realization, *Phys. Rev. A* **95**, 032318 (2017).